

THE BEHAVIOUR OF NICKEL AMALGAMS IN
PHOSPHORIC ACID SOLUTIONS

3

By

R. Abou Shahba, N.S. Hassan, A.S. Ahmed and
S.M. Roshdy*

Al-Azhar University for Girls, Faculty of Science,
Chemistry Department, Nasr City, Cairo, Egypt.

Abstract :

Nickel amalgams of varying concentrations were anodically oxidized galvanostatically in phosphoric acid solutions at 25°C. Two different oxidation patterns were distinguished. The first described the behaviour of the nickel amalgams in concentrated acid solutions (1.0 and 3.0 N H_3PO_4) and the second gave the behaviour of nickel amalgams in dilute acid solutions (0.1 N H_3PO_4). The oxidation curves in concentrated solutions showed regions for the charging of the anodic double layer, dissolution of nickel as Ni^{++} followed by its oxidation to NiO , formation of mercurous and mercuric phosphate, Ni_3O_4 and Ni_2O_3 which is oxidized further to NiO_2 before oxygen evolution.

With dilute solutions the oxidation curves revealed that, the charging of the anodic double layer, dissolution of Ni as Ni^{++} , and its oxidation to NiO as in concentrated phosphoric acid solutions,

was followed by a region of oscillations due to the consecutive formation and dissolution of mercurous and mercuric phosphate. The NiO formed at the early stages of passivity is then oxidized to Ni_3O_4 , Ni_2O_3 then NiO_2 before oxygen evolution.

The relation between the polarizing current, i , and the time of passivation, τ , was found to follow the following equation :

$$\text{Log } \tau = A - n \log i$$

where A and n are constants. The results indicate that the diffusion of nickel within the amalgam to the amalgam / electrolyte interface was mainly rate determining in the process of passivation.

The effect of temperature on the time of passivation of nickel amalgams in phosphoric acid solution was also investigated.

Introduction :

The chemical literature is rich with information regarding the oxidation and passivation of metallic alloys. Certain rules are put to explain and predict the beneficial or detrimental effects resulting from incorporating traces of one metal in the bulk of another. Little of such work is directed, however, to study of alloys in which mercury forms the main constituent.

Moreover, nickel and its alloys possess excellent corrosion resistance in a wide variety of environments. This naturally rises considerable interest in investigating the cause of passivity of nickel. Several techniques have been employed to characterize the nature and the thickness of the surface film⁽¹⁻²⁴⁾.

Therefore the main objective of this study was to investigate the composition of the film formed on a nickel amalgam electrode and throw more light on the mechanism leading to the electrode passivation.

Experimental :

The electrical cell and experimental details were similar to those given previously⁽²⁵⁾. The amalgam electrode was in the form of a small cup of 1.67 cm internal diameter, provided with a sealed platinum wire. The cathode was in the form of an auxiliary electrode with a sealed platinum contact. In order to avoid the contamination of the tested solution with the cathode products, the cathode was isolated from the electrolytic solution. This was achieved by auxiliary electrode in a special compartment fitted with a sintered - glass disk of medium porosity.

The potential of the working electrode was measured against a saturated calomel electrode. All potentials are referred to the reversible hydrogen electrode scale.

The amalgam of the electrodes were prepared electrolytically in situ from the acid plating baths having the following composition: 90 g. Ni SO₄. 7 H₂O, 30 g. NiCl₂. 6 H₂O, 16 g. (NH₄)₂SO₄, 30 ml H₃PO₄ and 4.5 g. NH₄Cl / L.

A known amount of solution was introduced into the electrode cup containing 1.5 ml of doubly distilled mercury and electrolysis was carried out with fixed

current 50 m.A./electrode for nickel with mercury acting as the cathode. The electrode area was 2.30 cm². The mercury and electrolyte were continuously stirred. Complete plating of the metal was marked by the brisk evolution of hydrogen gas from the surface of the electrode. Electrolysis was continued for a further 30 min. period. The amalgam was washed several times with doubly distilled water, and then dried with narrow strips of filter paper. Complete deposition of nickel was ascertained by atomic absorption analysis.

Amalgams varying in concentration between 0.6448×10^{-2} to 3.8557×10^{-2} wt% nickel were thus prepared. Orthophosphoric acid solution was used as testing media to prepare 3.0, 1.0 and 0.1 N solutions.

The results and analysis indicate that the nickel amalgam electrodes prepared in this manner have the following composition (Table 1.)

Table 1. Amalgams Electrode Composition :

Electrode No.	Ni solution, ml	wt-% Ni	Mole fraction
I	0.5	0.6448×10^{-2}	2.2615×10^{-3}
II	2.0	2.5738×10^{-2}	8.6965×10^{-3}
III	3.0	3.8557×10^{-2}	12.9880×10^{-3}

Results and Discussion :

Anodic and cathodic polarization curves for nickel amalgams with increasing metal content were traced in 0.1, 1.0 and 3.0 N - H_3PO_4 solutions at 25°C. For each amalgam and solution composition number of constant polarizing currents were applied to gain insight into the mechanism of passivation.

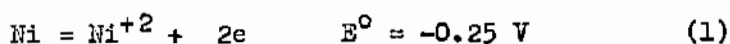
The results of the present investigation on the anodic behaviour of nickel amalgams in phosphoric acid solutions showed two different oxidation patterns. The first describes the behaviour of the nickel amalgams in concentrated acid solutions (1.0 and 3.0 N H_3PO_4) and the second gives the behaviour of these amalgams in dilute acid solutions (0.1 N H_3PO_4).

The behaviour of nickel amalgams in concentrated acid solutions :

Under a wide range of constant polarizing current densities and solution concentrations (1 and 3N H_3PO_4), nickel amalgams (electrode I, II and III) yield polarization curves which exhibit practically the same features.

Figs. (1,2) represent the potential - time curves of nickel amalgam electrodes (Electrode III and I) in 3.0 and in 1.0 N H_3PO_4 solutions respectively. It can

be seen that, the primary anodic process in the polarization curves represents the charging of the anodic double layer, then the Ni of the amalgam dissolves as Ni^{+2} along region (i) (showing no inflection) according to the following equation :



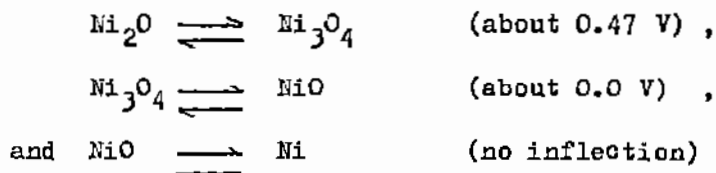
This reaction is considered for solid nickel electrode, however for nickel amalgams under consideration the reduction in the nickel atom activity must also be accounted for. As a fair approximation the activity of nickel in mercury could be set equal to its mole fraction χ_{Ni} which for 2.2615×10^{-3} and 12.988×10^{-3} wt - % Ni amalgam amounts to 0.64448×10^{-2} , 2.5738×10^{-2} and 3.8557×10^{-2} respectively.

Substitution of these values in the basic Nernst equation :

$$E = E^{\circ} + 0.059 \text{ pH} - 0.029 \log \chi_{Ni} \quad (2)$$

gave for the three amalgams in 0.1, 1, and 3 N- H_3PO_4 , values varying from -0.093 to -0.133 V. Formation of Ni^{+2} along this region (i), in the polarization curves corresponds to the first period of activity of nickel amalgams, which is then oxidized to NiO (region ii) showing no inflection also.

Formation of NiO along region ii was also reported by previous authors⁽¹⁰⁾ who reported that, by the galvanostatic technique, small constant c.d. causes the potential of nickel electrode to increase suddenly to a value that corresponds to the reversible NiO/Ni potential. Similar observations were also found by Besson⁽²¹⁾ upon his study on the anodic oxidation of nickel electrode in 6N - KOH solution by Rollet's method reported that, the equilibrium transformation which occurs together with the oxidation reduction potential (in V) determined at the points of inflection of the anodic potential-time curves were :



The formation of NiO along region (ii) was followed by five clear arrests. Along arrests (I) and (II), mercurous and mercuric phosphate were formed and the surface of the amalgam electrode was covered with a white deposit.

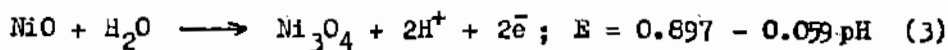
Evidence that mercurous and mercuric phosphate were formed during arrests I and II in the polarization curves can be arrived at, by consideration of Fig. (3)

in which pure mercury is oxidized in 1 N-H₃PO₄ acid under the same experimental conditions (the same current density, solution concentration and temperature).

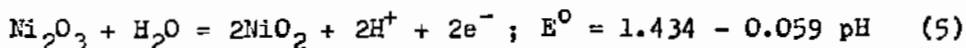
Further information for the formation of mercurous and mercuric phosphate along arrests I and II, respectively, was also confirmed by measuring the open circuit potential that arises from these salts on the surface of a clean doubly distilled mercury pool surface, where values of 625 and 675 mV. were obtained for mercurous and mercuric phosphate, respectively.

Due to the solubility of mercurous and mercuric phosphates in acids, an elongation of the step of formation of mercuric phosphate occurs, Fig. (1); and oscillations occur in the potential-time curve (specially in dilute solutions Fig.(4)) due to the continuous formation and dissolution of the salt layer.

Owing to the liquid nature of the electrode, the primary passivating film contained fissures and cracks which allowed the amalgam to come in contact with the solution and the nickelous oxide NiO formed at the first stage of passivity (region ii), would be oxidized to higher oxides along steps III and IV according to



Ni_2O_3 which is formed along step IV is further oxidized to NiO_2 along arrest V, according to the following reaction⁽²⁶⁾:

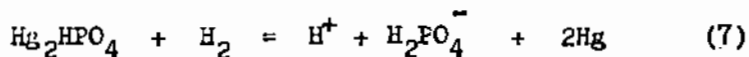
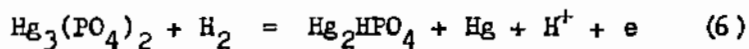


before finally the potential rises to oxygen evolution values.

These results are in agreement with those obtained by previous authors on solid nickel electrodes in sodium phosphate solution⁽¹⁷⁾. They suggested that the passive film on nickel electrode has a duplex structure consisting of NiO and Ni_3O_4 . At high potential NiO_2 was produced on top of the initial film.

Cathodic polarization curves were traced by reversing the polarizing currents when the potential was at oxygen evolution values (curve C, Figs. 1,2), so as to make the working electrode the cathode.

Three arrests appeared in the cathodic polarization curve. The first two corresponds to the reduction of mercuric and mercurous phosphate according to the following reactions.



Then reduction ^{of} NiO_2 to NiO took place along the third arrest before finally the potential drops to hydrogen evolution values.

Anodic decay curves obtained upon interrupting the polarizing current when the electrode was at oxygen evolution values (curve D, Figs. 1,2), indicated that the potential dropped directly to values corresponding to the system $\text{Hg}_3\text{PO}_4/\text{Hg}_2\text{HPO}_4$ where the potential remains constant thereafter.

The behaviour of nickel amalgams in dilute phosphoric acid solutions :

Quite interesting is the oxidation characteristics of nickel amalgams in dilute solutions. In Fig. (4) are shown the anodic polarization curves for (2.5738×10^{-2} wt. % Ni) in 0.1 N - H_3PO_4 acid. As indicated from the shapes of the anodic polarization curves (Fig. (4)); it can be seen that, the charging of the anodic double layer and dissolution of Ni as Ni^{++} , followed by its oxidation to NiO as mentioned before in concentrated phosphoric acid solutions (1 and 3 N) was followed by a region of oscillations which may probably be due to the fact that, the formed mercurous and mercuric phosphate are soluble in acid phosphate solutions⁽¹⁸⁾. The formed layers in these dilute solutions once formed

readily dissolve, and fluctuations occur in the anodic polarization curves due to the formation and breakdown of these salts at the first stages of passivity. After certain time the NiO formed at the early stages of passivity is then oxidized to Ni_3O_4 along step I in the polarization curve, (Fig. 4) which is then oxidized to Ni_2O_3 then NiO_2 along steps III and IV as given before in case of concentrated phosphoric acid solutions.

Relation between the polarizing current, i (μA) and time of passivation, τ (min) :

In order to gain further insight on the nature of the process that eventually leads to the electrode passivation (film formation), the relation between the polarizing current, i (μA) and time of passivation τ (min) was considered. Plots of these two variables (C.F. Fig. 5) for electrode III in 0.1, 1.0 and 3N H_3FO_4 solutions, gave almost parallel straight lines with slopes of -2 in excellent agreement with $n = 2$, predicted by Muller's empirical formula and Sand's equation for electrolysis with constant current (chronopotentiometry) (27). Similar observations were also found for electrode I and II in phosphoric acid solutions.

As seen from these curves (Fig. 5), the passivation of the different nickel amalgams in the examined solutions are satisfactorily represented by the relation

$$\text{Log } \tau = A - n \log i \quad (8)$$

where A and n are constants

In table (2) the values of the constants A and n of relation (7) are grouped.

Table (2) :

Values of the constants A and n in relation (7).

Solution	Electrode No.	A	n
3N H ₃ PO ₄	I	7.49	2
	II	7.80	2
	III	7.89	2
1N H ₃ PO ₄	I	7.51	2
	II	7.65	2
	III	7.69	2
0.1N H ₃ PO ₄	I	6.40	2
	II	6.47	2
	III	7.18	2

From the results of the present investigation the passivation of nickel amalgams in H_3PO_4 solutions appears to be largely governed by the rate of diffusion of nickel atoms to the electrode / electrolyte interface.

Furthermore, it is readily seen from Fig. 6 (electrode III in 0.1, 1.0 and 3N H_3PO_4 solutions) that the value of $i \tau^{1/2}$ is almost constant (for one and the same concentration of amalgam) as the current density was varied. The same results were also obtained for electrode I and II in phosphoric acid solutions.

Consideration of the theoretical relations underlying the process of electrolysis at controlled current can reveal the exact nature of the diffusing ion which participates in the formation of the passivity film. For the product $i \tau^{1/2}$, the term passivation index is here suggested since it gives a clear understanding of the process of passivation.

Effect of temperature on the time of passivations of nickel amalgams in phosphoric acid solution :

The results of the anodic polarization of 2.5738×10^{-2} wt% nickel amalgam in 1N- H_3PO_4 solution at different temperatures are show diagrammatically in

Fig. (7). The polarizing current density was $261 \mu\text{A}/\text{cm}^2$.

As can be seen from these curves, the time of passivation increases with rise of temperature. Since the potential - time curves are analogous in shape at higher and lower temperatures, save for the increased time of passivation at higher temperatures, hence, the effect of temperature may be accounted for, as due to the increased solubilities of the layers initially present or anodically formed on the electrode surface, therefore, the time needed for the passivation of the electrode greatly increases.

- (1) A.K.N. Reddy and B. Rao.: Canadian Journal of Chemistry, 47, 2687 (1969).
- (2) W. Machu and A. Ragheb: Werkstoffe und Korrosion, 12, 429 (1953).
- (3) U. Ebersbach, K. Schwabe and P. Köning: Electrochimica Acta, 14, 773-81 (1969).
- (4) W.J. Müller : Monatsh, 54, 559 (1927).
- (5) W.J. Müller, H.K. Cameron and W. Machu : Monatch, 52, 73 (1932).
- (6) K. Goergi : Z. Electrochemistry, 38, 714 (1932).
- (7) N. Sato and G. Okamoto: Trans Japan Institute of Metals: 2, 113-19 (1961), C.A. 56, 11343 i (1962).
- (8) E.P. Schoch: Journal Trans American Chemical Society, 14, 99-112 (1908).
- (9) L. Transtad : Zphysik Chemistry, 142, 241 (1929).
- (10) T.S. De Gromoboy and L.L. Shreir: Electrochemica Acta, 11, 895 - 904 (1966).
- (11) K. Schwabe: Electrochimica Acta, 3, 186 (1960), C.A. 55, 3237 a (1961).
- (12) J.R. Myers: Corrosion 21(9), 277-87 (1965).
- (13) N.F. Myrphy and O.C. Baharat: C.A. 53, 2674e (1959).

- (14) J. Matulis and J. Bubelis: C.A. 26, 2506b (1965).
- (15) E. Yeager, F. Hovorka, H.L. Kronenberg and J.C. Banter: C.A., 59, 7158e (1963).
- (16) A. Hickling and J.E. Spice: Trans Farad. Society, 43, 762 - 69 (1947), C.A., 42, 5365f (1948).
- (17) M. Okuyama and S. Haruyama: Corrosion Science, 41, 1 (1974).
- (18) G.Y. Chao, Z. Szklarska Smialowska and D.D. Macdonald: Journal Electroanalytical chemistry, 131, 289 - 297 (1982).
- (19) I.P. Dezider'eva and F.F. Faizullin: C.A. 54, 63629 (1960).
- (20) Davies and Barker: Journal Electrochimica Acta, 11, 895 - 904 (1966).
- (21) J. Besson : C.A. 40, 6005⁷ (1964).
- (22) M.N. Ronzhin and A.I. Golubev: C.A. 64, 189549 (1966).
- (23) A. Smith : "Inorganic and Theoretical chemistry". J.W. Müller, D.Sc., F.R.S. Volume IV Longmans, Green and Co. London, New York, Toronto.
- (24) G.Y. Chao, Z. Szklarska Smialowska and D.D. Macdonald: Journal Electroanalytical chemistry, 131, 279 - 287 (1982).

Women's Coll. Ann. Rev.
Vol. 15 (1990).

- (25) H.M. Sammour, L.A. Kamel and S.M. Roushdi :
Corrosion Science, 13, 939-48 (1973).
- (26) M. Pourbaix: Atlas of Electrochemical Equilibria
in aqueous solutions. Pergamon Press Ltd.
(1966).
- (27) H. J.S. Sand: Phil. Mag., 1 (1901).

Fig. 1 : Anodic, Cathodic and Decay Polarization of
Electrode III of Ni - Amalgam in 3N-H₃PO₄.
—○— o.d. 600 $\mu\text{A}/\text{Cm}^2$ —×— c.d. 522 $\mu\text{A}/\text{cm}^2$
—△— o.d. 435 $\mu\text{A}/\text{Cm}^2$ —●— c.d. 348 $\mu\text{A}/\text{cm}^2$
—□— c.d. 261 $\mu\text{A}/\text{Cm}^2$

Fig. 2 : Anodic, Cathodic and Decay Polarization of
Electrode I of Ni-Amalgam in 1N-H₃PO₄.
—○— c.d. 435 $\mu\text{A}/\text{Cm}^2$ —×— o.d. 348 $\mu\text{A}/\text{cm}^2$
—△— c.d. 304 $\mu\text{A}/\text{Cm}^2$ —●— o.d. 260 $\mu\text{A}/\text{cm}^2$
—□— c.d. 174 $\mu\text{A}/\text{Cm}^2$

Fig. 3 : Anodic, Cathodic and Decay Polarization of
Hg in 1N-H₃PO₄ , c.d. = 261 $\mu\text{A}/\text{cm}^2$.

Fig. 4 : Anodic, Cathodic and Decay Polarization of
Electrode II of Ni - Amalgam in 0.1N-H₃PO₄
—○— o.d. 435 $\mu\text{A}/\text{Cm}^2$ —×— c.d. 348 $\mu\text{A}/\text{cm}^2$
—△— o.d. 304 $\mu\text{A}/\text{Cm}^2$ —●— c.d. 260 $\mu\text{A}/\text{cm}^2$

Fig. 5 : Log i - Log τ Relation for Electrode III in :
—○— 3.0N-H₃PO₄ —×— 1.0N-H₃PO₄
—●— 0.1N-H₃PO₄

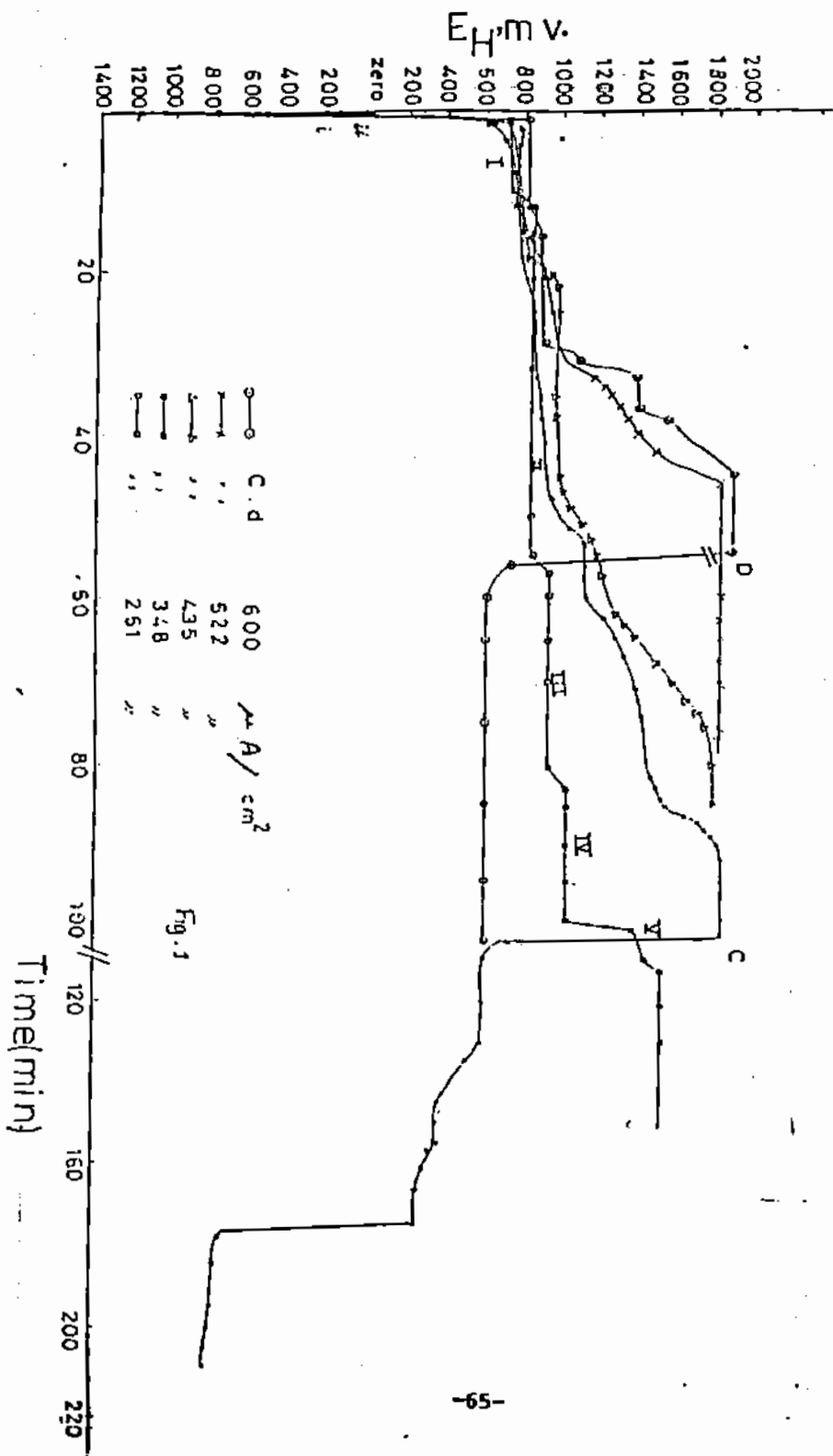
Fig. 6 : Relation between $i\tau^{1/2} \times 10^3$ and i (μA) for
Electrode III in :

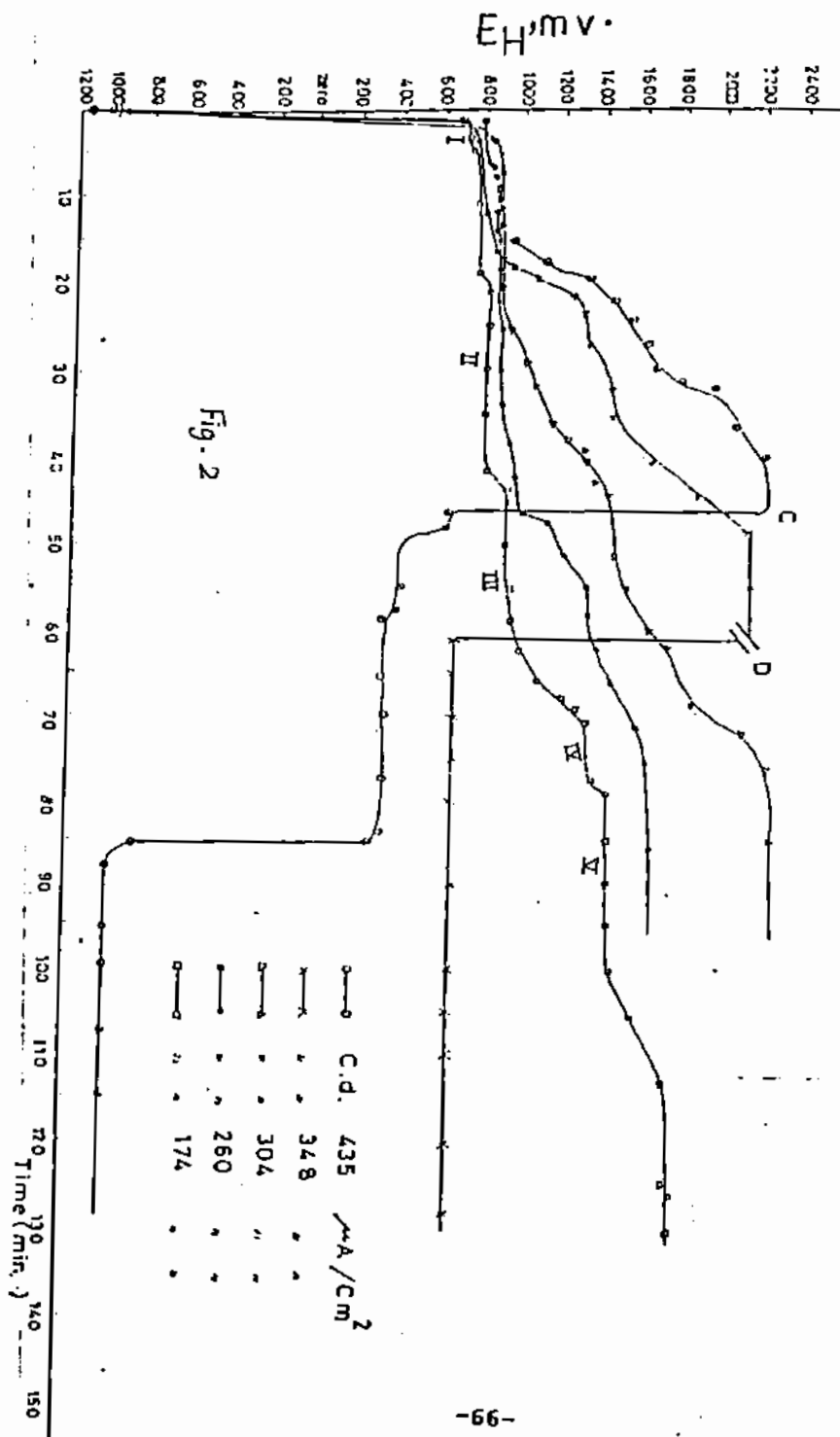
—○— 3.0N-H₃PO₄ —x— 1.0N-H₃PO₄
—●— 0.1N-H₃PO₄

Fig. 7 : Effect of Temperature in Electrode II in :

1.0N-H₃PO₄ , c.d. 261 mA/cm²

—○— 45°C —x— 35°C —△— 30°C
—●— 20°C —□— 10°C





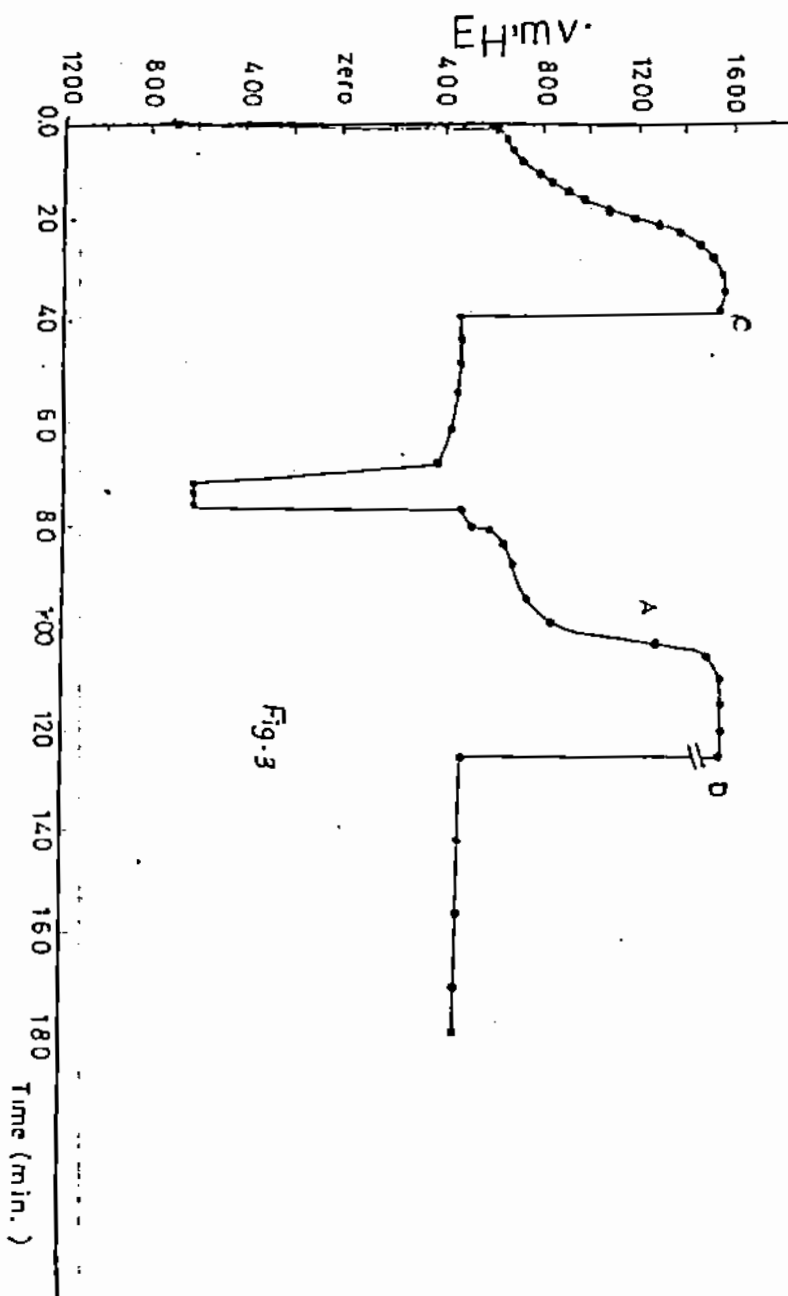
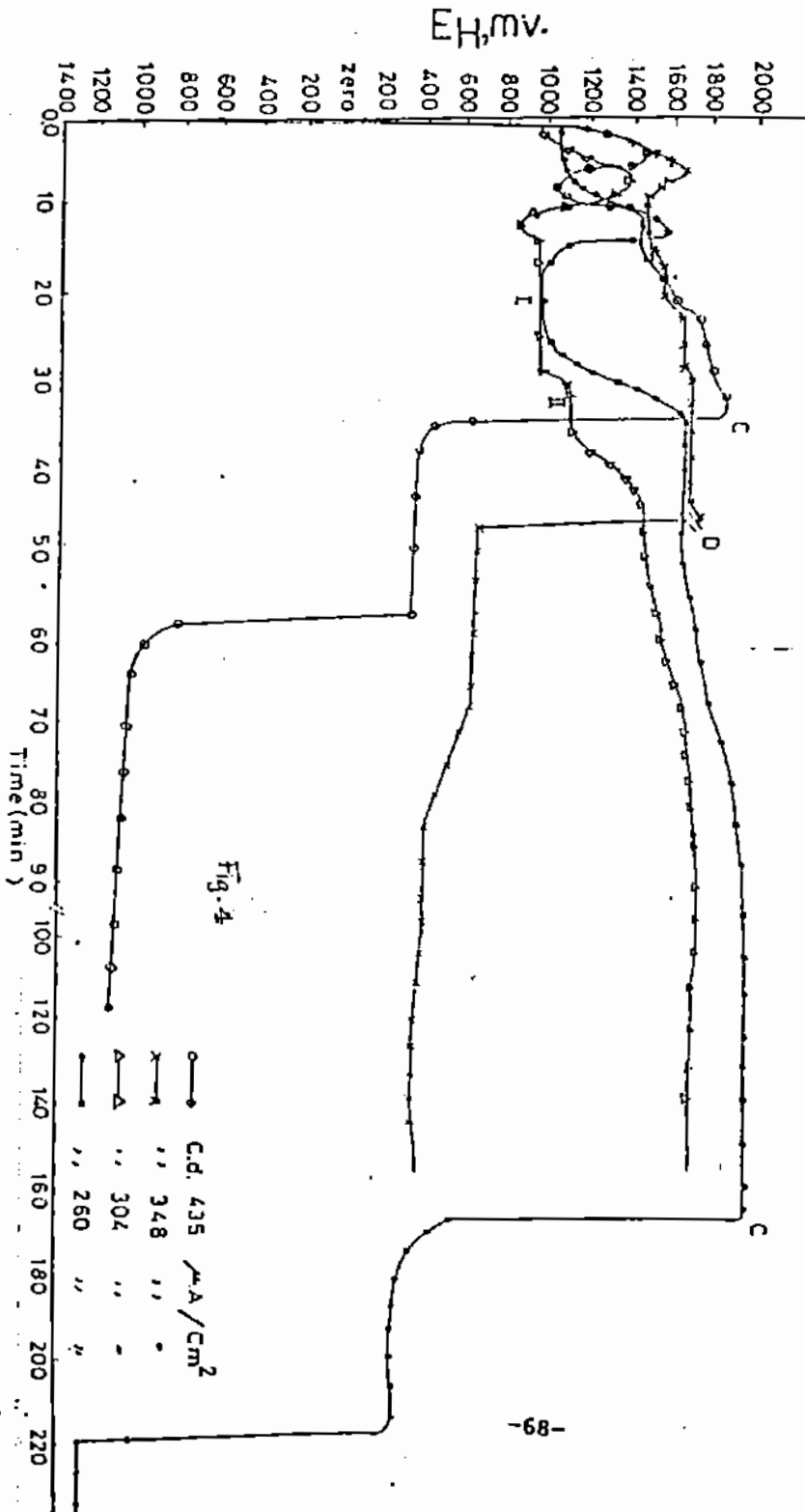


Fig. 3



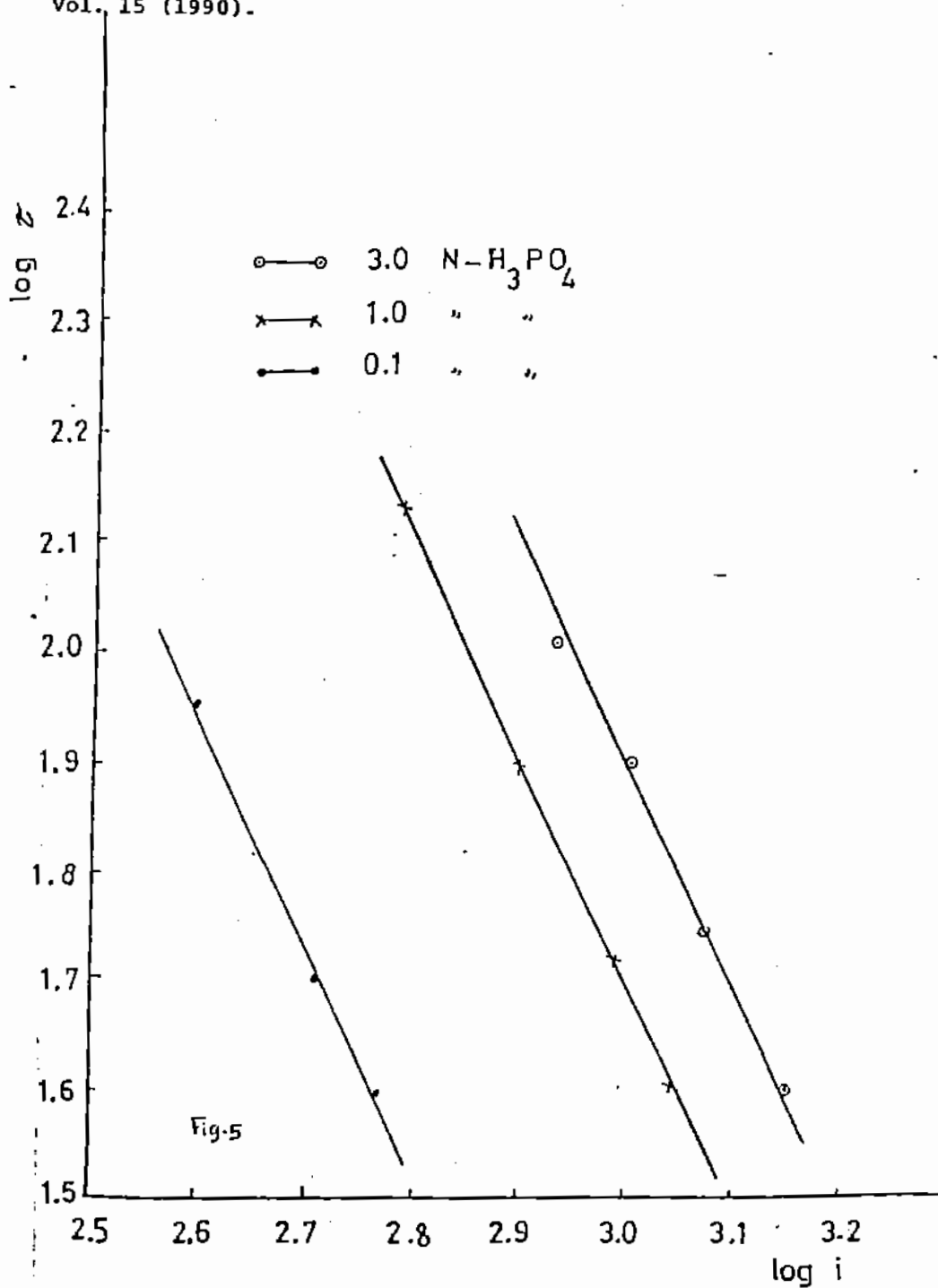


Fig-5

